Neuronal plasticity features are independent of neuronal holding membrane potential

Roni Vardi[1], Yael Tugendhaft[2] and Ido Kanter[1,2,*]

[1]Gonda Interdisciplinary Brain Research Center, Bar-Ilan University, Ramat-Gan, 52900, Israel.
[2]Department of Physics, Bar-Ilan University, Ramat-Gan, 52900, Israel.

[*]Corresponding author email: ido.kanter@biu.ac.il

Dynamical reversible neuronal features in vitro are typically examined using a fixed holding membrane potential, imitating the physiological conditions of intact brains in an awake state. Here, a set of neuronal plasticity features in synaptic blocked cultures are found to be independent of the holding membrane potential in the range [-95, -50] mV. Specifically, dendritic maximal firing frequency and its absolute refractory period are independent of the holding membrane potential. In addition, the stimulation threshold is also independent of the holding membrane potential in neurons that do not show membrane depolarization in response to sub-threshold stimulations. These robust dendritic plasticity features are a prerequisite for neuronal modeling and for their utilization in interconnected neural networks to realize higher-order functionalities.

Introduction

The neuronal resting membrane potential stems from an imbalance of electrical charges between the interior and surroundings of the soma. In a steady-state condition in the vicinity of a neuron, the resting membrane potential is assumed to be around -70 mV; however, it can transitorily vary above and below this value as a function of excitatory and inhibitory presynaptic signals[1,2]. In addition, a common scenario for oscillating membrane potentials is the Up and Down states[3] under anesthesia or sleep[4,5]. These broadband oscillations are typically of the sub-Hertz range[6], where the Down state is close to the resting membrane potential and the Up state is a few millivolts below the neuronal threshold. These oscillations are commonly assumed to be absent in neuronal cultures; however, transitory periods of several seconds that deviate from the resting membrane potential have also been observed in spontaneously active neuronal cultures[7].

Understanding neuronal plasticity features as a function of membrane potential is important for neuronal modeling as well as for understanding its role in the formation of higher-order functionalities in interconnected neural networks. Experimental examination of the connection between neuronal plasticity features and the holding membrane potential (HMP) requires stabilization of the neuronal membrane potential for many minutes. Although neuronal dynamics are characterized by visible long-term memory extending over seconds[8], the realization of time-independent membrane potentials over minutes is not possible. Nevertheless, a patched neuron within a synaptic-blocked culture enables control of the HMP over timescales of tens of minutes and the characterization of its plasticity features.

The presented results indicate the robustness of neuronal plasticity features for different HMPs, suggesting that their regulatory source is outside the soma, most likely at the dendrites. Such reversible neuronal plasticity features include the neuronal maximal firing frequency[8], neuronal absolute refractory period[9-11], and neuronal stimulation threshold. Their independence from the HMP indicates that dendritic plasticity[8,9,12-16] dominates their quantitative features.

The experimental setup consisted of synaptic blocked neuronal cultures plated directly onto substrate-integrated multi-electrode arrays[16]. This enabled multiple complex

extracellular stimulations and recordings from a microelectrode array simultaneously with patch-clamp recordings of a single neuron.

Results

Independency of maximal firing frequency on the HMP

The first type of experiment measured the sensitivity of neuronal responsiveness to above-threshold stimulations as a function of the HMP. For a sufficiently high stimulation frequency, f, the neuronal response latency (NRL) increases by several milliseconds with an increasing number of stimulations until the neuron enters the intermittent phase (Fig. 1(a)). This phase is characterized by fluctuations in the NRL around a fixed value, together with the appearance of neuronal response failures, such that the average firing frequency, f_c, is independent of $f > f_c$ [8,17]. This critical frequency, f_c, which varies among neurons, was demonstrated to be independent of the HMP (Fig. 1(b)). Quantitatively, the results indicated that the average deviation of f_c with HMP $\sim -90\,mV$ or $\sim -50\,mV$ relative to f_c with $HMP = -70\,mV$ is small (1.05 average and 0.14 standard deviation, $n = 24$, Fig. 1(c)). In addition, no systematic trends were observed for HMP above/below $-70mV$ (Fig. 1(c) and Material and Methods). Hence, the emergence of neuronal response failures and their average statistics are unlikely to be attributable to somatic processes. The independence of f_c from the HMP, together with previously reported results[18] on the anisotropic properties of the NRL and f_c, strongly indicate that these phenomena stem from dendritic plasticity[19,20].

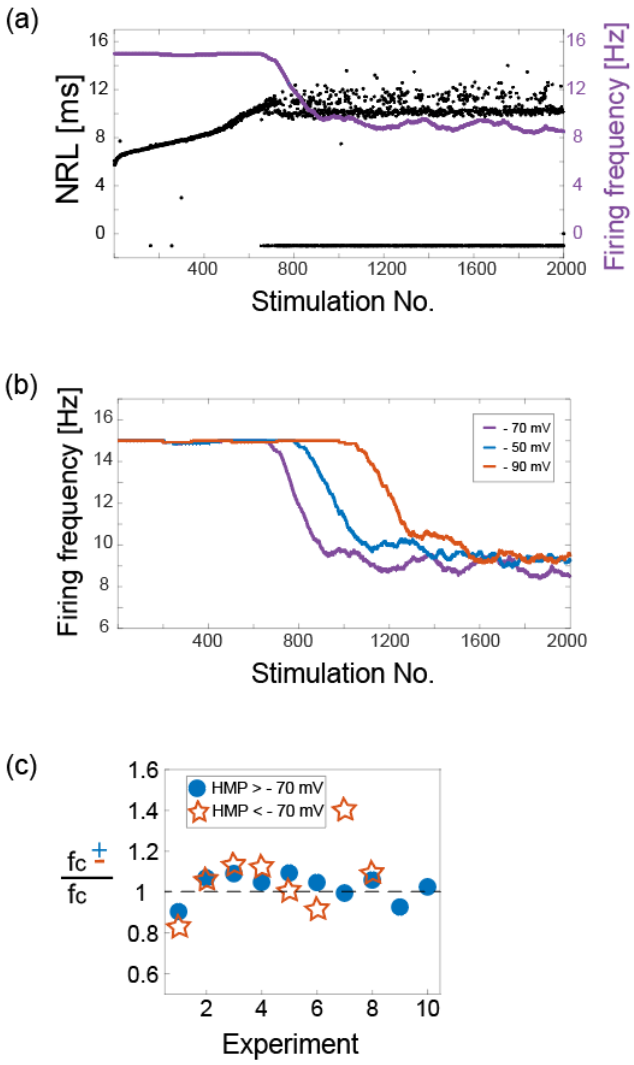

Fig. 1. Independency of maximal firing frequency on the HMP. (a) Neuronal response latency (NRL) of a neuron with HMP=$-70\ mV$ stimulated at 15 Hz (black, response failures are denoted at NRL=-1) and its firing frequency averaged over a sliding window of 200 stimulations (purple). The neuron enters the intermittent phase after ~ 700 stimulations. (b) The firing frequency, averaged over a sliding window of 200 stimulations, for the neuron in (a), stimulated at 15 Hz, using different HMP: $-90\ mV$ (orange), $-70\ mV$ (purple), and $-50\ mV$ (blue). (c) The relative deviation of the firing frequency at the intermittent phase, $\frac{f_c^-}{f_c} \equiv f_c\,(HMP < -70\ mV)/f_c\,(HMP = -70mV)$ (orange stars, $n = 8$, average=1.07, std=0.17), and $\frac{f_c^+}{f_c} \equiv f_c\,(HMP > -70\ mV)/f_c\,(HMP = -70mV)$ (blue dots, $n = 16$, average=1.04, std=0.135).

Independency of ARP on the HMP

The second type of experiment compared the neuronal absolute refractory period (ARP)[10,11] for different HMP. To measure the ARP, pairs of extracellular stimulations with monotonically increasing intra-pair time-lags were applied to a patched neuron[9] (Fig. 2(a)-(b)). The stimulating extracellular electrode and the amplitude of the stimulations were preselected to ensure reliable responses at low-frequency stimulations. In addition, pairs of stimulations were separated by at least one-second time-lags, which were much greater than the intra-pair time-lags, to ensure a non-overlapping effect between consecutive pairs. The deviation of ARP with HMP $\sim -90\,mV$ or $\sim -50\,mV$ from ARP at $HMP = -70\,mV$ is presented ($n = 41$, Fig. 2(c)). Note that the averaged ARP at $-70\,mV$ ($n = 24$, Fig. 2(c)), measured with $0.5\,ms$ resolution, is $\sim 5.54\,ms$ [9], and the standard deviation of ARP with different HMP is below $1\,ms$ (Fig. 2(c)). Hence, the results clearly indicate that ARP is almost independent of HMP.

In advanced experiments, ARP as a function of the HMP of a single neuron was measured independently for two different extracellular stimulating electrodes. The results indicate two distinct ARPs, one for each electrode, almost independent of the HMP (e.g., measuring the ARP using one extracellular electrode at HMP= -75/-65 mV resulted in 6/5.5 ms, respectively, and in 4.5/4.5 ms when using a different extracellular electrode). These results exemplify the neuronal anisotropic nature, which has been previously demonstrated for a fixed HMP[9,21], and strongly support the assumption that ARP originates from a dendritic mechanism.

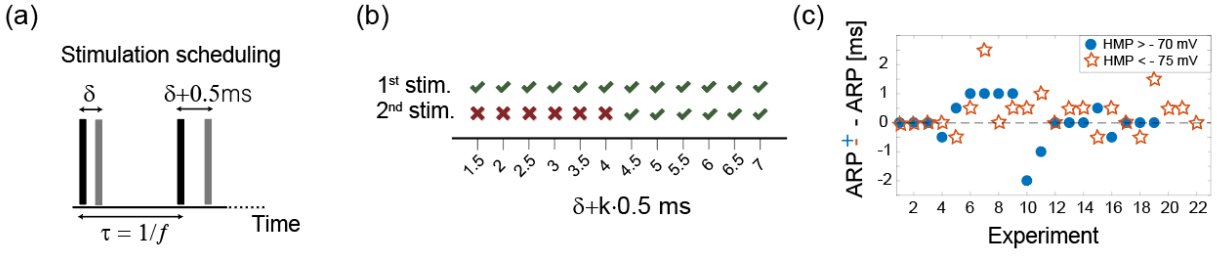

Fig. 2. Independency of ARP on the HMP. (a) Scheme of the extracellular stimulation scheduling for measuring the neuronal refractory period. Pairs of extracellular stimulations given at frequency f=1 Hz with monotonically increasing internal time-lags, $\delta + k \cdot 0.5\,ms$, where δ is the first time-lag and k is the pair's number. (b) The stimulation scheduling with $\delta = 1.5\,ms$, resulting in a

$4.5\,ms$ ARP for different HMP: $-75mV, -53\,mV,$ and $-90\,m$. Evoked spike/response failure for each pair of stimulations is denoted by green-v/red-x, respectively. (c) The deviation in ms of $ARP^{-} - ARP \equiv ARP(HMP < -75\,mV) - ARP(HMP = -70mV)$ (orange stars, $n = 22$, average=0.34 ms, std=0.68) and similarly for $ARP^{+} - ARP \equiv ARP(HMP > -70\,mV) - ARP(HMP = -70mV)$ (blue dots, $n = 19$, average=0.052 ms, std= 0.74).

Independency of stimulation threshold on the HMP

The third type of experiment examined the neuronal stimulation threshold as a function of the HMP using the following procedure: For a given neuron and HMP, the amplitude of extracellular stimulations with a fixed duration decreased until a transition from evoked spikes to their disappearance was observed[9]. The minimal measured stimulation amplitude generating reliable evoked spikes was defined as the neuronal stimulation threshold.

Two types of neuronal responses were observed. In the first type, sub-threshold stimulations did not cause transitory increases in membrane potential (Fig. 3(a)). The absence of membrane depolarization was consistent even when the stimulation strength was a few millivolts below the threshold, excluding the possibility that depolarization appeared close to the threshold only. In contrast, the second type exhibited depolarization for sub-threshold stimulations (Fig. 3(b)), similar to the effect of the excitatory postsynaptic potential (EPSP) in unblocked cultures[12,13]. These two types of neuronal responses exhibited quantitatively different behaviors as a function of HMP (Fig. 3).

For neurons demonstrating depolarization for sub-threshold stimulations (second type), the stimulation threshold depended on the HMP ($n = 8$). Specifically, for a higher HMP, the stimulation threshold decreased by typically ≤ 100 mV (Fig. 3(b)). This tendency was expected because the depolarization amplitude effectively reduced the neuronal threshold. However, this effect was absent for the first type of neuron, in which the threshold was independent of the HMP (Fig. 3(a)).

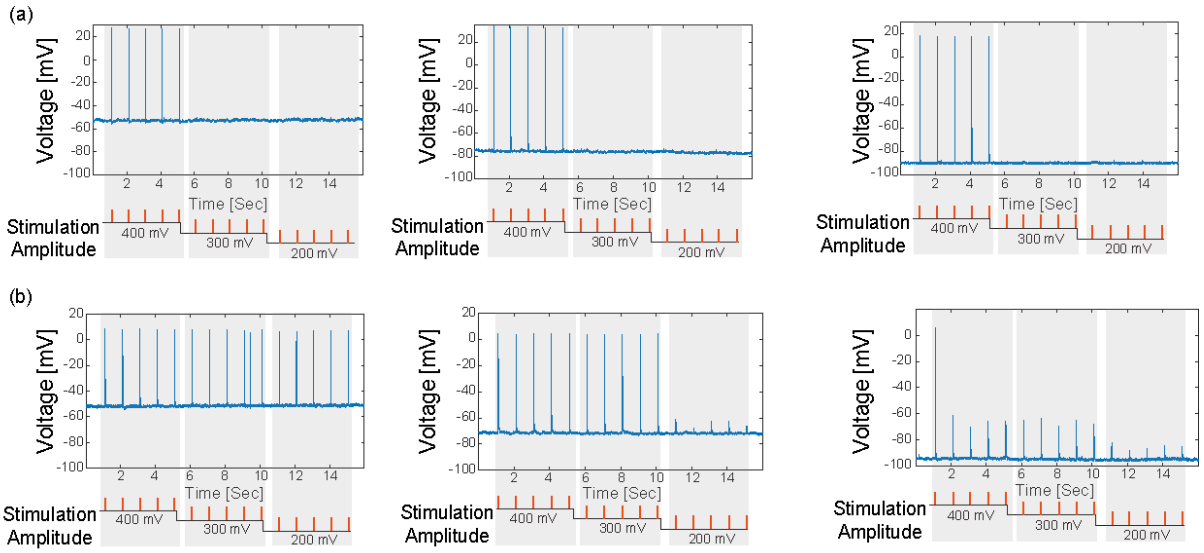

Fig. 3. Independency of stimulation threshold on the HMP in neurons without depolarization for sub-threshold stimulation. (a) An example (among $n = 7$ examined neurons that demonstrated the same behavior) of the independency of the stimulation threshold on the HMP ($\sim -50\ mV$, left; $\sim -70\ mV$, middle; $\sim -90\ mV$, right) for the first type of neuronal responses that do not exhibit depolarization for sub-threshold stimulation amplitudes. Five simulations are given for each stimulation amplitude to ensure reliable responses. (b) An example (among $n = 8$ examined neurons that demonstrated the same behavior) of the dependency of the stimulation threshold on the HMP ($\sim -50\ mV$, left; $\sim -70\ m$V, middle; $\sim -90\ mV$, right) for the second type of neuronal responses that exhibit depolarization for sub-threshold stimulation amplitudes. Five simulations are given for each stimulation amplitude to ensure reliable responses.

We note that the first and second types of neuronal responses were observed in hundreds of examined neurons at HMP $= -70\ mV$ only, where both could coexist in a single neuron stimulated from different extracellular electrodes. The first type seemed to be more frequent in our experiments at HMP $= -70\ mV$; however, its verification requires further research, and the results may differ among specific types of cortical neurons. Nevertheless, it is evident that the responses of the second type of neurons vary between Up and Down states, but responses of the first type remain unaffected. Hence, the decrease in the activity of a neural network composed of the first and second types is expected to decrease with an increasing fraction of second-type neurons.

For the first type of neuronal responses, while increasing the stimulation amplitude, the neuron jumps discontinuously from a no-response to an evoked spike state, without any prior signal on the measured membrane potential. Such a discontinuous transition can occur in fundamental discrete (quantum) physical microscopic systems[22] but is unexpected for macroscopic biological realities, that is, membrane potential. Nevertheless, this might stem from the phenomenon of dendritic spike generation[23-25].

Conclusions

Recently, a neuron was demonstrated to function as a multiple-threshold unit, where each dendrite could generate a different spike waveform with its own dendritic threshold[16]. When the dendritic threshold is crossed, a dendritic spike propagates to the soma; the soma then relays the influx of dendritic spikes to the axon, while amplifying or reshaping the spike waveform[25]. It is important to distinguish between two conditions where the amplitude of the dendritic spike[25] is either greater or smaller than the membrane threshold. If the amplitude is greater, the dendritic spike activates the membrane potential to further relay the dendritic spike to the axon. Transitory depolarization of the membrane potential is absent because a signal activating a dendritic spike always triggers the membrane potential and generates a somatic spike. This scenario is the origin of neuronal responses without depolarization, which is the first type of response. In contrast, when the dendritic spike amplitude is lower than the membrane threshold, its influx into the membrane generates visible depolarization[25]. However, the mechanism of the generation of somatic spikes under this scenario is unclear. This understanding deserves further research. However, we propose two possible reasons for this. The first possible scenario is that the dendritic spike amplitude varies with stimulation amplitude[25]. The second is the generation of several dendritic spikes that are almost synchronized at different dendritic sites. These dendritic spikes merge along the dendritic tree toward the soma and form a combined amplitude above the membrane threshold.

The anisotropic features of neuronal reversible plasticity have recently been discovered to govern many neuronal phenomena, including neuronal response latency[15], response failures[8,26], absolute refractory periods[9,21] and spike waveforms[16]. The timescale of these reversible plasticities is broadband, ranging from microseconds to tens of seconds, and

their anisotropic properties depend on the soma stimulation route. In addition, irreversible plasticity in the form of fast dendritic adaptation has been observed in other types of experiments[12,13]. The current study demonstrates the robustness of the presented neuronal phenomena to different HMPs from different perspectives to support dendritic reversible plasticity. The independency of the examined dynamic neuronal features in the HMP suggests that they are controlled by processes outside the soma. This finding, together with the anisotropic properties, highlights dendritic plasticity as the main mechanism. The observation of a large fraction of neurons without membrane depolarization for sub-threshold stimulation questions the origin of spike generation. The results suggest that spikes are generated at the dendrites and then relayed to the axon via the soma[25], which functions mainly as a nonlinear hub amplifier.

Materials and Methods

Data analysis: Analyses were performed in a MATLAB environment (MathWorks, Natwick, MA, USA). The recorded data from the MEA (voltage) was filtered by convolution with a Gaussian that has a standard deviation (STD) of 0.1 ms. Evoked spikes were detected by threshold crossing, −10 mV, using a detection window of [0.5, 20] ms following the beginning of an electrical stimulation.

Stimulation and recording—MEA: An array of 60 Ti/Au/TiN extracellular electrodes, 30 μm in diameter, and spaced 500 μm from each other (Multi-Channel Systems, Reutlingen, Germany) was used. The insulation layer (silicon nitride) was pre-treated with polyethyleneimine (0.01% in 0.1 M Borate buffer solution). A commercial setup (MEA2100-60-headstage, MEA2100-interface board, MCS, Reutlingen, Germany) for recording and analyzing data from 60-electrode MEAs was used, with integrated data acquisition from 60 MEA electrodes and 4 additional analog channels, integrated filter amplifier and 3-channel current or voltage stimulus generator. Each channel was sampled at a frequency of 50k samples/s, thus the recorded action potentials and the changes in the neuronal response latency (NRL) were measured at a resolution of 20 μs. Mono-

phasic square voltage pulses were used, in the range of [−900, −100] mV and [100, 2000] µs.

Recording—Patch Clamp: The electrophysiological recordings were performed in whole cell configuration utilizing a Multiclamp 700B patch clamp amplifier (Molecular Devices, Foster City, CA). The cells were perfused with extracellular solution consisting of (mM): NaCl, 140; KCl, 3; $CaCl_2$, 2; $MgCl_2$, 1; HEPES, 10 (Sigma-Aldrich Corp. Rehovot, Israel), supplemented with 2 mg/ml glucose (Sigma-Aldrich Corp. Rehovot, Israel); pH, 7.3; and osmolarity adjusted to 300–305 mOsm. The patch pipettes had resistances of 3–5 MOhm after filling with a solution containing (in mM): KCl, 135; HEPES, 10; glucose, 5; MgATP, 2; GTP, 0.5 (Sigma-Aldrich Corp. Rehovot, Israel); pH, 7.3; and osmolarity adjusted to 285–290 mOsm. After obtaining the giga-ohm seal, the membrane was ruptured and the cells were subjected to fast current clamp by injecting an appropriate amount of current to adjust the membrane potential to about −70 mV. The changes in neuronal membrane potential were acquired through a Digidata 1550 analog/digital converter using pClamp 10 electrophysiological software (Molecular Devices, Foster City, CA). The acquisition started upon receiving the TTL trigger from MEA setup. The signals were filtered at 10 kHz and digitized at 50 kHz. The cultures mainly consisted of pyramidal cells. For patch clamp recordings, pyramidal neurons were intentionally selected based on their morphological properties.

MEA and Patch Clamp synchronization: The experimental setup combines multi-electrode array, MEA 2100, and patch clamp. The multi-electrode array is controlled by the MEA interface boarded and a computer. The patch clamp sub-system consists of several microstar manipulators, an upright microscope (Slicescope-pro-6000, Scientifca), and a camera. Stimulations and recordings are implemented using multiclamp 700B and Digidata 1550A and are controlled by a second computer. The recorded MEA/patch data is saved on the computers respectively. The time of the MEA system is controlled by a clock placed in the MEA interface board and the time of the patch subsystem is controlled by a clock placed in the Digidata 1550A. The relative timings are controlled by triggers sent from the MEA interface board to the Digidata using leader-laggard configuration.

Extracellular electrode selection: For the extracellular stimulations in the performed experiments an extracellular electrode out of the 60 electrodes was chosen by the following procedure. While recording intracellularly, all 60 extracellular electrodes were stimulated serially at 2 Hz and above-threshold, where each electrode is stimulated several times. The electrodes that evoked well-isolated, well-formed spikes were used in the experiments. After choosing the extracellular electrode we verify that the stimulation is not antidromic, by verifying that the NRL is several ms long. In addition, the NRL is verified to increase by several ms with the number of stimulations, and in case that the stimulation frequency is above the critical frequency, f_C, response failures occur. We report only experiments where the leak of the patched neuron was stable.

Neuronal response latency: The neuronal response latency (NRL) is defined as the time-lag between a stimulation pulse onset and its corresponding evoked spike measured by crossing a threshold of -20 mV.

Animals: All procedures were in accordance with the National Institutes of Health Guide for the Care and Use of Laboratory Animals and Bar-Ilan University Guidelines for the Use and Care of Laboratory Animals in Research and were approved and supervised by the Bar-Ilan University Animal Care and Use Committee.

Culture preparation: Cortical neurons were obtained from newborn rats (Sprague-Dawley) within 48 h after birth using mechanical and enzymatic procedures. The cortical tissue was digested enzymatically with 0.05% trypsin solution in phosphate-buffered saline (Dulbecco's PBS) free of calcium and magnesium, and supplemented with 20 mM glucose, at 37°C. Enzyme treatment was terminated using heat-inactivated horse serum, and cells were then mechanically dissociated mostly by trituration. The neurons were plated directly onto substrate-integrated multi-electrode arrays (MEAs) and allowed to develop functionally and structurally mature networks over a time period of 2–4 weeks in vitro, prior to the experiments. The number of plated neurons in a typical network was in the order of 1,300,000, covering an area of about ~5 cm^2. The preparations were bathed

in minimal essential medium (MEM-Earle, Earle's Salt Base without L-Glutamine) supplemented with heat-inactivated horse serum (5%), B27 supplement (2%), glutamine (0.5 mM), glucose (20 mM), and gentamicin (10 g/ml), and maintained in an atmosphere of 37°C, 5% CO_2 and 95% air in an incubator. All experiments were performed at a temperature of 37°C.

Synaptic blockers: Experiments were conducted on cultured cortical neurons that were functionally isolated from their network by a pharmacological block of glutamatergic and GABAergic synapses. For each culture, 20 µl of a cocktail of synaptic blockers were used, consisting of 10 µM CNQX (6-cyano-7-nitroquinoxaline-2, 3-dione), 80 µM APV (DL-2-amino-5-phosphonovaleric acid), and 5 µM Bicuculline methiodide. This minimal cocktail completely blocked the spontaneous network activity. The blockers were added until no spontaneous activity was observed both in the MEA and in the patch clamp recording. In addition, repeated extracellular stimulations did not provoke the slightest cascades of neuronal responses.

References

1 Doan, T. N. & Kunze, D. L. Contribution of the hyperpolarization-activated current to the resting membrane potential of rat nodose sensory neurons. *The Journal of physiology* **514**, 125-138 (1999).

2 Yamada-Hanff, J. & Bean, B. P. Persistent sodium current drives conditional pacemaking in CA1 pyramidal neurons under muscarinic stimulation. *Journal of Neuroscience* **33**, 15011-15021 (2013).

3 Tukker, J. J., Beed, P., Schmitz, D., Larkum, M. E. & Sachdev, R. N. Up and down states and memory consolidation across somatosensory, entorhinal, and hippocampal cortices. *Frontiers in systems neuroscience* **14**, 22 (2020).

4 Steriade, M., Nunez, A. & Amzica, F. A novel slow (< 1 Hz) oscillation of neocortical neurons in vivo: depolarizing and hyperpolarizing components. *Journal of neuroscience* **13**, 3252-3265 (1993).

5 Wilson, C. J. & Kawaguchi, Y. The origins of two-state spontaneous membrane potential fluctuations of neostriatal spiny neurons. *Journal of neuroscience* **16**, 2397-2410 (1996).

6 Sanchez-Vives, M. V. & McCormick, D. A. Cellular and network mechanisms of rhythmic recurrent activity in neocortex. *Nat Neurosci* **3**, 1027-1034 (2000).

7 Vardi, R., Goldental, A., Sardi, S., Sheinin, A. & Kanter, I. Simultaneous multi-patch-clamp and extracellular-array recordings: Single neuron reflects network activity. *Sci Rep-Uk* **6**, 36228, doi:10.1038/srep36228 (2016).

8 Vardi, R. *et al.* Neuronal response impedance mechanism implementing cooperative networks with low firing rates and μs precision. *Front Neural Circuit* **9**, 29 (2015).

9 Sardi, S. *et al.* Long anisotropic absolute refractory periods with rapid rise times to reliable responsiveness. *Physical Review E* **105**, 014401 (2022).

10 Hodgkin, A. L. & Huxley, A. F. A quantitative description of membrane current and its application to conduction and excitation in nerve. *The Journal of physiology* **117**, 500-544 (1952).

11 Berry, M. & Meister, M. Refractoriness and neural precision. *Advances in neural information processing systems* **10** (1997).

12 Sardi, S. *et al.* Brain experiments imply adaptation mechanisms which outperform common AI learning algorithms. *Sci Rep-Uk* **10**, 1-10 (2020).

13 Sardi, S. *et al.* Adaptive nodes enrich nonlinear cooperative learning beyond traditional adaptation by links. *Sci Rep-Uk* **8**, 5100, doi:10.1038/s41598-018-23471-7 (2018).

14 Brama, H., Goldental, A., Vardi, R., Stern, E. & Kanter, I. Hours of high-frequency stimulations reveal intracellular neuronal trends in vivo. *EPL (Europhysics Letters)* **116**, 46002 (2016).

15 Vardi, R., Timor, R., Marom, S., Abeles, M. & Kanter, I. Synchronization with mismatched synaptic delays: A unique role of elastic neuronal latency. *EPL (Europhysics Letters)* **100**, 48003 (2012).

16 Sardi, S., Vardi, R., Sheinin, A., Goldental, A. & Kanter, I. New Types of Experiments Reveal that a Neuron Functions as Multiple Independent Threshold Units. *Scientific reports* **7**, 18036 (2017).

17 Brama, H., Goldental, A., Vardi, R., Stern, E. & Kanter, I. Hours of high-frequency stimulations reveal intracellular neuronal trends in vivo. *Europhys Lett* **116**, 46002 (2016).

18 Vardi, R., Goldental, A., Sheinin, A., Sardi, S. & Kanter, I. Fast reversible learning based on neurons functioning as anisotropic multiplex hubs. *EPL (Europhysics Letters)* **118**, 46002 (2017).

19 Sardi, S. *et al.* Dendritic learning as a paradigm shift in brain learning. *ACS chemical neuroscience* **9**, 1230-1232 (2018).

20 Hodassman, S., Vardi, R., Tugendhaft, Y., Goldental, A. & Kanter, I. Efficient dendritic learning as an alternative to synaptic plasticity hypothesis. *Scientific Reports* **12**, 1-12 (2022).

21 Vardi, R., Tugendhaft, Y., Sardi, S. & Kanter, I. Significant anisotropic neuronal refractory period plasticity. *EPL (Europhysics Letters)* **134**, 60007 (2021).
22 Sakurai, J. J. & Commins, E. D. (American Association of Physics Teachers, 1995).
23 Castañares, M. L., Bachor, H.-A. & Daria, V. R. Analyzing Branch-specific Dendritic Spikes Using an Ultrafast Laser Scalpel. *Front Phys* **8**, 600971 (2020).
24 Schiller, J., Major, G., Koester, H. J. & Schiller, Y. NMDA spikes in basal dendrites of cortical pyramidal neurons. *Nature* **404**, 285-289 (2000).
25 Gidon, A. *et al.* Dendritic action potentials and computation in human layer 2/3 cortical neurons. *Science* **367**, 83-87 (2020).
26 Vardi, R., Goldental, A., Sheinin, A., Sardi, S. & Kanter, I. Fast reversible learning based on neurons functioning as anisotropic multiplex hubs. *Europhysics Letters* **118**, 46002 (2017).